Accepted Manuscript

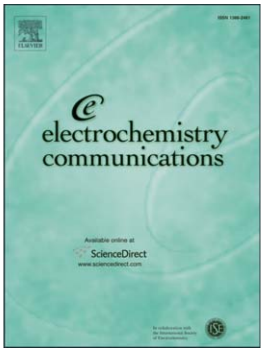

In situ FTIR spectroscopic study of ethanol oxidation on Pt(111)/Rh/Sn surface. The anion effect

Marcia E. Paulino, Luiza M.S. Nunes, Ernesto R. Gonzalez, Germano Tremiliosi-Filho

PII: S1388-2481(14)00406-8
DOI: doi: 10.1016/j.elecom.2014.12.025
Reference: ELECOM 5357

To appear in: *Electrochemistry Communications*

Received date: 16 October 2014
Revised date: 9 December 2014
Accepted date: 22 December 2014

Please cite this article as: Marcia E. Paulino, Luiza M.S. Nunes, Ernesto R. Gonzalez, Germano Tremiliosi-Filho, In situ FTIR spectroscopic study of ethanol oxidation on Pt(111)/Rh/Sn surface. The anion effect, *Electrochemistry Communications* (2014), doi: 10.1016/j.elecom.2014.12.025

In situ FTIR spectroscopic study of ethanol oxidation on Pt(111)/Rh/Sn surface. The anion effect

Marcia E. Paulino, Luiza M.S. Nunes, Ernesto R. Gonzalez, Germano Tremiliosi-Filho*

Instituto de Química de São Carlos, Universidade de São Paulo
Avenida Trabalhador São-Carlense 400
13569-590 - São Carlos, SP, Brazil

** Corresponding author. tel.: +55 16 33739933; fax: +55 16 33739951.*
e-mail address: germano@iqsc.usp.br (G.Tremiliosi-Filho).

Abstract

In situ Fourier Transform Infrared (FTIR) spectroscopy was used to study the anion effect in ethanol oxidation on Pt (111) surface modified by rhodium and tin, Pt(111)/Rh/Sn. The *in situ* FTIR spectra showed that ethanol oxidation reaction pathway is strongly influenced by the nature of the electrolyte anion. In perchloric and sulfuric acid electrolytes were observed the formation of acetaldehyde, acetic acid and CO_2, however in phosphoric acid the acetic acid is not observed. The sulfuric acid is the most favorable electrolyte for acetaldehyde and CO_2 formation

Keywords: in situ FTIR, ethanol electro-oxidation, Pt(111)/Rh/Sn, sulfuric acid, perchloric acid, phosphoric acid.

1. Introduction

In recent years there has been a growing interest in the study of ethanol oxidation because of its potentiality for application in fuel cells [1-5].

The electrocatalyst can strongly influence the ethanol oxidation reaction pathway [6-11]. Platinum is the most studied electrocatalyst and it is well known that this reaction on platinum electrode [12,13] can occur by different mechanistic routes, as: (i) ethanol oxidation to acetaldehyde, with further oxidation to acetic acid; (ii) ethanol and acetaldehyde oxidatizing to CO and additional fragments, CH_x, that can be futher oxidized to CO_2 [12].

Several metals have been added to Pt to improve the electrocatalytic activity [14-16]. Pt/Rh alloy shows hability to break the C-C bond and also promote the break of the C-H bond following the CO_2 formation [7, 12].

Pt/Sn promotes the cleavage of O-H bond of the water molecule forming oxygenated species that assist the ethanol oxidation reaction [4, 5, 15,17].

Ternary Pt-Rh-SnO_2/C alloy exhibits good performance for ethanol oxidation at low potential forming CO_2 as major product [18].

In this context, Pt(111) modified by subsequente rhodium and tin adatom depositions was used as a model surface to improve it electrocatalytic activity. The interaction of anions of supporting electrolyte and the ethanol is equally importante [19-23]. Thus, the anion effect (sulfate, perchlorate and phosphate) was studied by *in situ* FTIR spectroscopy during the ethanol oxidation reaction on Pt(111)/Rh/Sn.

2. Experimental

All solutions were prepared with Millipore-MilliQ® water (18.2 MΩ cm). $HClO_4$ (Sigma Aldrich), H_2SO_4 (Merck Suprapur) and H_3PO_4 (Mallinckrodt) acids were used as supporting electrolyte solutions in the concentration of 0.1 mol L^{-1}. Solutions of $Rh_2(SO_4)_3$ (Premion) and $SnSO_4$ (Vetec) in a concentration of $5x10^{-6}$ mol L^{-1} in 0.1 mol L^{-1} of acid media were used for deposition of sub-monolayer of Rh and Sn on Pt(111) surface. Ethanol (J. T. Baker) and acetaldehyde (Sigma Aldrich) were used in a concentration of 0.5 mol L^{-1}. High pure grade Argon (White Martins) was used to deareate the solutions. All experiments were carried out at room temperature of 20 ± 1 ^{o}C.

A reversible hydrogen electrode (RHE) in different acid supporting electrolyte solutions was used as reference systems and a platinum foil as a counter electrode. Pt(111) single crystal electrode (MaTeck, 1 cm diameter) modified with rhodium and tin was used as working electrode.

Pretreament of the single crystal and it transfer to the electrochemical cell were described elsehere [24].

Three electrochemical cells were used. The first one was employed to evaluated the quality of the single crystal surface and the purity of the supporting electrolyte; the second one, was used to perform electrochemical deposition of rodhium on Pt(111); and finally the third cell, was used for electrochemical deposition of tin on Pt (111)/Rh.

Bare Pt(111) surface was characterized by cyclic voltammetry using a meniscus configuration at potential range between 0.06 V and 0.85 V vs RHE in acid media. Rhodium deposition on Pt(111) was performed by cycling (six cycles) in the potential region 0.07 V – 0.8 V vs. RHE in $5x10^{-6}$ mol L^{-1} $Rh_2(SO_4)_3$ solution in 0.1 mol L^{-1} acid medium at a sweep rate of 0.01 V s^{-1}. Tin deposition on Pt(111)/Rh was performed by cycling (five cycles) at potential range from 0.1 to 0.6 V vs. RHE in 5x10^{-6} mol L^{-1} $SnSO_4$ solution in 0.1 mol L^{-1} acid medium at a sweep rate of 0.01 V s^{-1}.

The electrochemical measurements were performed with a Solartron 1285 potentiostat. The FTIR equipment was a Nexus 670 – Nicolet equipped with a MCT detector. Typically, *in situ* FTIR spectroscopy measurements were performed simultaneously with cyclic voltammetry at potentials from 0.06 V to 0.9 V vs RHE at 2 mV s^{-1}. The *in situ* spectroelectrochemical system consisted of ZnSe IR transparent window attached to the bottom of the cell. Spectra were computed from the average of 16 interferograms, and the spectral resolution was set to 8 cm^{-1}. Reflectance spectra were calculated as the ratio (R/R_o) between a sample (R) and a reference (R_o) spectra. Positive bands represent loss and negative bands is due to gain of species at the sampling potential

3. Results and discussion

Rhodium and tin coverages on Pt(111) electrode were calculated as θ_{Rh} = 0.66 and θ_{Sn} = 0.25 [25, 26]. Fig.1(A) shows voltammetric cycles recorded during ethanol oxidation on the Pt(111) and Pt(111)/Rh/Sn electrodes in different acid electrolytes. The lowest onset potential for ethanol oxidation was observed in sulfuric and phosphoric acid electrolytes. In perchloric acid electrolyte, the Pt(111) without modification shows high ethanol oxidation current density than the Pt(111)/Rh/Sn electrode.

Fig. 1(B) shows *in situ* FTIR spectra recorded during ethanol oxidation on Pt(111)/Rh/Sn in $HClO_4$ electrolyte. The formation of acetaldehyde, acetic acid and CO_2 [27,28] bands at *ca* 930, 1282 and 2341 cm^{-1}, respectively, confirm the ethanol oxidation [9-12]. The band at 2983 cm^{-1} is attributed to the C-H fragment [4], which appears at the potential of 0.86 V vs. RHE. This C-H fragment can be correlated with the $=COH—CH_3$, $—OCH_2—CH_3$, $—CO—CH_3–CH_2$ species formed during the course of ethanol oxidation at high potentials as suggested by Iwasita and collaborators [13, 29]. The band at 1110 cm^{-1} is atributed to Cl-O stretching [30] correlated to ClO_4^-. The band at 1716 cm^{-1} is atributed to C=O stretching [28] correlated to COOH and/or CHO which ocurrs in potentials higher than 0.56 V vs. RHE. The inset shows a low intensity band characteristic of the C–O stretch of a CHO group of the aldehyde at ca. 1258 cm^{-1}. Nevertheless, this band was not observed on bare Pt(111) [29]. Thus, the Rh and Sn deposit promoted the appearing of this band.

In H_2SO_4 electrolyte the main products formed from ethanol oxidation on Pt(111)/Rh/Sn were similar to those obtained in $HClO_4$ electrolyte. In H_3PO_4 solution, the acetic acid band at ca. 1282 cm^{-1} is absent at the *in situ* FTIR spectra (data not shown).

In general, during the ethanol oxidation reaction it is usually observed the formation of adsorbed carbon monoxide on bare platinum catalyst surface [12, 29]. However, in this study CO is not formed on Pt(111)/Rh/Sn indicating that this specie is not a reaction intermediate, independently of the anion.

The acetaldehyde and CO_2 band intensities were chose for monitoring the anion effect of the supporting electrolyte on the ethanol oxidation, see Figs. 1(C) and 1(D). The acetaldehyde, Fig. 1(C), and CO_2, Fig. 1(D), band intensities were direct calculated from the bands at ca. 930 and 2341 cm^{-1}, respectively.

The potentials observed for the initial formation of acetaldehyde occur in the order $H_2SO_4 < HClO_4 < H_3PO_4$, see Fig.1(C),

In the case of CO_2 formation, see Fig. 1(D), the initial potentials occur at 0.46 V vs RHE in both H_2SO_4 and H_3PO_4 electrolytes, with higher band intensities in H_2SO_4. In $HClO_4$ electrolyte, the lowest CO_2 band intensity, exhibit an initial formation potential at 0.66V vs RHE. Kowal et al. [17] observed in this same electrolyte an initial potential of 0.48 V vs. RHE on $RhSnO_2$/Pt(111) prepared by thermal decomposition at 200 ˚C of $SnCl_4$ on Rh/Pt(111).

In summary, the best performance for the ethanol oxidation is observed in the H_2SO_4 electrolyte due to: (i) higher band intensities associated to formation of acetaldehyde and CO_2, and (ii) lowest initial formation potentials, 0.36 V vs. RHE for acetaldehyde and 0.46 V vs. RHE for CO_2, see Figs. 1(C) and 1(D). It is important to observe that the initial formation potential for CO_2 in H_2SO_4 is the same one observed in H_3PO_4 electrolyte, however, the band intensity in phosphoric acid is much less intense than in sulfuric acid. Additionaly, the acetaldehyde start to appears only at high potentials, ca. 0.76 V vs RHE in H_3PO_4, and coincides with the phosphate desorption potential [31, 32]. For comparison, the initial potentials for acetaldehyde and CO_2 formation in $HClO_4$ electrolyte, are 0.56 V vs. RHE and 0.66 V vs. RHE, respectively, see Fig. 1(C) and 1(D).

During the ethanol oxidation, its adsorption occurs at 0.3 V on Pt with a subsequent formation of the following adsorbed species: $=COH—CH_3$, $—OCH_2—CH_3$, $—CO—CH_3$ and —CO, that can be futher oxidized to CO_2, according to DEMS results [29]. Thus, it is possible to infer that similar adsorbed species, except CO_{ads}, may be formed in H_2SO_4, H_3PO_4 and $HClO_4$

electrolytes, and can be oxidized to CO_2, without goes through the CO_{ads}. The Rh/Pt, Sn/Pt, prepared by deposition of Rh or Sn on Pt surface and $RhSnO_2$/Pt(111), prepared by thermal decomposition of $SnCl_4$ on Rh/Pt(111), favor the C–C bond break with formation of adsorbed CO [8,16,17] that is further oxidized to CO_2. This mechanistic step occurs at a low onset potential, ca 0.3 V vs RHE, and involves surface adsorbed oxygen donor as, adsorbed OH, following a well established Langmuir-Hinshelwood mechanism. On the other hand, for the Pt(111)/Rh/Sn the CO_2 is formed without previous formation of adsorbed CO, see Fig. 1(B). Additionally, the initial potentials for CO_2 formation on this material are 150 mV in H_2SO_4 and H_3PO_4 and 350 mV in $HClO_4$ more positives than the observed for Pt/Rh, Pt/Sn and $RhSnO_2$/Pt(111) electrode. These are evidences that other kind of reaction intermediates as, e.g. $=COH—CH_3$ and $—CO—CH_3$, are involved in the CO_2 formation. Acetaldehyde formation on Pt(111)/Rh/Sn electrode occurs in lower potentials than the ones for CO_2 in H_2SO_4 and $HClO_4$ electrolytes, indicating that the first mechanistic step of the ethanol oxidation involves the formation of acetaldehyde, that is futher oxidized to CO_2. However, the formation of acetaldehyde in H_3PO_4 medium follows a different mechanistic route that possible involves the specie $=COH—CH_3$, before CO_2 formation.

The ethanol oxidation in phosphoric acid solution on Pt(111)/Rh/Sn prepared in: (a) phosphoric acid solution and, (b) sulfuric acid solution, showed similar behavior in terms of acetaldehyde and CO_2 band intensities, see Figs 1(C) and 1(D) (open and closed triangles). These results suggest that the anion used in the electrolyte for the electrode deposition does not exerce any influence on the Rh and Sn distribution on Pt(111) electrode.

Figure 1(E) exhibits the band intensities calculated at 1282 cm^{-1} for the acetic acid formation on Pt(111)/Rh/Sn electrode during the ethanol oxidation. The formation of this reaction product was observed only in H_2SO_4 and $HClO_4$ electrolytes. Acetic acid is a natural oxidation product resulted from acetaldehyde oxidation and involves 2 electrons in this mechanistic step [18]. In both eletrolytes, the initial formation potentials occur at the same potential, 0.66 V vs. RHE. The band intensities are similar and increase with the potential augmentation.

The proposed mechanism in H_2SO_4 and $HClO_4$ involves the C—H dissociation of the α–C with formation of adsorbed acetaldehyde, that can be futher oxidized to acetic acid or CO_2:

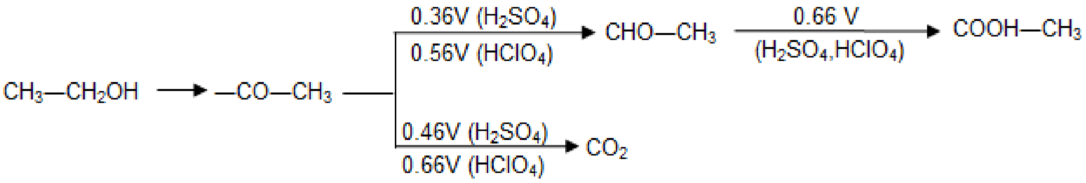

The FTIR measurements in H_3PO_4 show that the acetic acid generation is negligible during ethanol oxidation yielding only CO_2 and acetaldehyde with a predominant formation of CO_2 in low potentials:

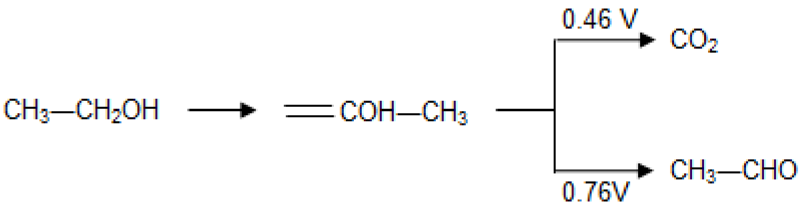

Fig. 2(A) shows voltammetric curves of acetaldehyde oxidation on Pt(111)/Rh/Sn electrode in different electrolytes. The initial acetaldehyde oxidation potential values observed in voltammograms (Fig. 2(A)) were in accordance with acetaldehyde bands order observed in *in situ* FTIR ethanol oxidation spectra in each acid electrolyte medium, see Figs. 2 (B), 2(C) and 2(D). In the phosphoric acid electrolyte (Fig. 2(B)), the acetaldehyde band intensity increase up to potential of 1.2 V vs. RHE. Similar behavior is observed in perchloric and sulfuric acid, Figs. 2(C) and 2(D), respectively.

4. Conclusions

The anion effect was evaluated during the formation of acetaldehyde, acetic acid and CO_2 by *in situ* FTIR spectroscopy during ethanol oxidation reaction on Pt(111)/Rh/Sn electrode. The highest band intensity and the lowest formation potential for acetaldehyde and CO_2 was obtained in sulfuric acid.

The adsorbed CO was not detected as a reaction intermediate in all studied electrolytes. In sulfuric and perchloric acids the acetaldehyde was formed previously the appearance of CO_2. However, in phosphoric acid the production of CO_2 starts in 0.46 V vs RHE while the acetaldehyde shows up in much higher potential, 0.76 V vs RHE. It was concluded that the phosphate anions compete for adsorption sites with ethanol showing strong influence in the reaction pathway. Additionally, in this electrolyte was not observed formation of acetic acid during the ethanol oxidation reaction.

Two different mechanisms were proposed according to the anion effect in the ethanol oxidation reaction. In sulfuric and perchloric acids, the mechanism involves the acetaldehyde adsorption as the first oxidation step, while in phosphoric acid, the ethanol is direct oxidized to CO_2 at low potentials and also to acetaldehyde in high potentials.

Acknowledgments

Financial supports: Fundação de Amparo à Pesquisa do Estado de São Paulo (FAPESP - process (2012/18807-5) and Conselho Nacional de Desenvolvimento Científico e Tecnológico (CNPq – process 150885/2012-1).

References

[1] L. An, T.S. Zhao, R. Chen, Q.X. Wu, A novel direct ethanol fuel cell with high power density, J. Power Sources 196 (2011) 6219-6222.

[2] S. Rousseau, C. Coutanceau, C. Lamy, J.-M. Léger, Direct ethanol fuel cell (DEFC): electrical performances and reaction products distribution under operating conditions with different platinum-based electrodes, J. Power Sources 158 (2006) 18-24.

[3] S. Song, P. Tsiakaras, Recent progress in direct ethanol proton exchange membrane fuel cells (DE-PEMFCs), Appl. Catal. B: Environ. 63 (2006) 187-193.

[4] C. Lamy, S. Rousseau, E.M. Belgsir, C. Coutanceau, J.-L. Léger, Recent progress in the direct ethanol fuel cell: development of new platinum-tin electrocatalysis, Electrochim. Acta 49 (2004) 3901-3908.

[5] C. Lamy, E.M. Belgsir, J.-M. Léger, Electrocatalytic oxidation of aliphatic alcohols: application to the direct alcohol fuel cell (DAFC), J. Appl. Electrochem. 31 (2001) 799-809.

[6] E. Antolini, Catalysts for direct ethanol fuel cells, J. Power Sources 170 (2007) 1-12.

[7] F.H.B. Lima, E.R. Gonzalez, Ethanol electro-oxidation on carbon-supported Pt-Ru, Pt-Rh and Pt-Ru-Rh nanoparticles, Electrochim. Acta 53 (2008) 2963-2971.

[8] J.P.I Souza, S.L. Queiroz, K. Bergamaski, E.R. Gonzalez, F.C. Nart, Electro-oxidation of ethanol on Pt, Rh, and PtRh electrodes. A study using DEMS and in –situ FTIR techniques, J. Phys. Chem. B 106 (2002) 9825-9830.

[9] G.A. Camara, R.B. de Lima, T. Iwasita, The influence of PtRu atomic composition on the yields of etanol oxidation: a study by in situ FTIR spectroscopy, J. Electroanal. Chem. 585 (2005) 128-131.

[10] A.A. Abd-El-Latif, E. Mostafa, S. Huxter, G. Attard, H. Baltruschat, Electrooxidation of ethanol at polycrystalline and platinum stepped single crystals: a study by differential electrochemical mass spectrometry, Electrochim. Acta 55 (2010) 7951-7960.

[11] G.A. Camara, T. Iwasita, Parallel pathways of ethanol oxidation: the effect of ethanol concentration, J. Electroanal. Chem. 578 (2005) 315-321.

[12] F. Colmati, G. Tremiliosi-Filho, E.R. Gonzalez, A. Berná, E. Herrero, J.M. Feliu, Surface structure effects on the electrochemical oxidation of ethanol on platinum single crystal electrodes, Faraday Discuss. 140 (2009) 379-397.

[13] X.H. Xia, H.-D. Liess, T. Iwasita, Early stages in the oxidation of ethanol at low index single crystal platinum electrodes, J. Electroanal. Chem. 437 (1997) 233-240.

[14] H. Massong, H. Wang, G. Samjeské, H. Baltruschat, The co-catalytic effect of Sn, Ru and Mo decorating steps of Pt(111) vicinal electrode surfaces on the oxidation of CO, Electrochim. Acta 46 (2000) 701-707.

[15] H. Zhao, J. Kim, B.E. Koel, Adsorption and reaction of acetaldehyde on Pt(111) ans Sn/Pt(111) surface alloys, Surf. Sci. 538 (2003) 147-159.

[16] V.D. Colle, J. S. Garcia, G. Tremiliosi-Filho, E. Herrero, J. M. Feliu, Electrochemical and spectroscopic studies of ethanol oxidation on Pt stepped surfaces modified by tin adatoms, Phys. Chem. Chem. Phys. 13 (2011) 12163-12172.

[17] A. Kowal, M. Li, M. Shao, K. Sasaki, M.B. Vukmirovic, J. Zhang, N.S. Marinkovic, P. Liu, A.I. Frenkel, R.R. Adzic, Ternary Pt/Rn/SnO_2 electrocatalysis for oxidizing ethanol to CO_2, Nat. Mater. 8 (2009) 325-330.

[18] M. Li, A. Kowal, K. Sasaki, N. Marinkovic, D. Su, E. Korach, P. Liu, R.R. Adzic, Ethanol oxidation on the ternary Pt-Rh-SnO_2 electrocatalysts with varied Pt:Rh:Sn ratios, Electrochim. Acta 55 (2010) 4331- 4338.

[19] J. Clavilier, D. Armand, S.G. Sun, M. Petit, Electrochemical adsorption behavior of platinum stepped surfaces in sulphuric acid solutions, J. Electroanal. Chem. 205 (1986) 267-277.

[20] E. Herrero, K. Franaszczuk, A. Wieckowski, Electrochemistry of methanol at low index crystal planes of platinum: an integrated voltammetric and chronoamperometric study, J. Phys. Chem. 98 (1994) 5074-5083.

[21] Q. He, X. Yang, W. Chen, S. Mukerjee, B. Koel, S. Chen, Influence of phosphate anion adsorption on the kinetics of oxygen electroreduction on low index Pt(hkl) single crystals, Phys. Chem. Chem. Phys. 12 (2010) 12544-12555.

[22] N.M. Marković, R.R. Adžić, B.D. Cahan, E.B. Yeager, Structural effects in electrocatalysis: oxygen reduction on platinum low index single-crystal surfaces in perchloric acid solutions, J. Electroanal. Chem. 377 (1994) 249-259.

[23] M. Weber, I.R. de Moraes, A.J. Motheo, F.C. Nart, In situ vibrational spectroscopy analysis of adsorbed phosphate species on gold single crystal electrodes, Colloids Surf. A, 134 (1998) 103 - 111.

[24] J. Clavilier, R. Faure, G. Guinet, R. Durant, Preparation of monocrystalline Pt microelectrodes and electrochemical study of the plane surfaces cut in the direction of the {111} and {110} planes, J. Electroanal. Chem. 107 (1980) 205 - 209.

[25] R. Goméz, J. M. Feliu, Rhodium adlayers on Pt(111) monocrystalline surfaces. Electrochemical behavior and electrocatalysis. Eletrochim. Acta 44 (1998) 1191-1205.

[26] H. Massong, H. Wang, G. Samjeské, H. Baltruschat, The co-catalytic effect of Sn, Ru and Mo decoring steps of Pt(111) vicinal electrode surfaces on the oxidation of CO. Electrochim. Acta 46 (2000) 701-707.

[27] S.-C. Chang, L.-W.H. Leung, M.J. Weaver, Metal crystallinity effects in electrocatalysis as probed by real-time FTIR spectroscopy: electrooxidation of formic acid, methanol, and ethanol on ordered low-index platinum surfaces, J. Phys. Chem. 94 (1990) 6013-6021.

[28] G. Socrates, Infrared Characteristic Group Frequencies, Wiley, New York, 1996.

[29] T. Iwasita, E. Pastor, A dems and FTir spectroscopic investigation of adsorbed ethanol on polycrystalline platinum, Electrochim. Acta 39 (1994) 531-537.

[30] K. Nakamoto, Infrared and Raman Spectra of Inorganic and Coordination Compounds, Wiley, New York, 1986.

[31] R. Gisbert, G. García, M.T.M. Koper, Adsorption of phosphate species on poly-oriented Pt and Pt(1 1 1) electrodes over a wide range of pH, Electrochim. Acta 55 (2010) 7961–7968.

[32] J. Mostany, P. Martínez, V. Climent, E. Herrero, J.M. Feliu,Thermodynamic studies of phosphate adsorption on Pt(111) electrodes surfaces in perchloric acid solutions, Electrochimica Acta 54 (2009) 5836-5843.

Figure Captions:

Figure 1. (A) Cyclic voltammograms for ethanol oxidation, 0.5 mol L^{-1}, in 0.1 mol L^{-1} H_3PO_4, H_2SO_4 and $HClO_4$, at 10 mV s^{-1}, on Pt(111) (black line) and Pt(111)/Rh/Sn (gray line). **(B)** *In situ* FTIR spectra recorded during ethanol oxidation, 0.5 mol L^{-1}, in 0.1 mol L^{-1} $HClO_4$ electrolyte on Pt(111)/Rh/Sn electrode. Insert: Bands of CHO at *ca* 1258 cm^{-1} and COOH at *ca* 1282 cm^{-1}. **(C)** acetaldehyde, **(D)** carbon dioxide and **(E)** acetic acid band intensities as a function of potential in 0.1 mol L^{-1} acid electrolytes: (o) H_2SO_4, (□) $HClO_4$ and (Δ, ▲) H_3PO_4. The empty and full triangle symbols corresponde to Pt(111)/Rn/Sn prepared in phosphoric and sulfuric acid, respectively.

Figure 2. (A) Voltammetric profiles for acetaldehyde oxidation, 0.5 mol L^{-1}, on Pt(111)/Rh/Sn, recorded at 10 mV s^{-1}, in 0.1 mol L^{-1} H_2SO_4 (solid line), $HClO_4$ (dotted line) and H_3PO_4 (dashed line). *In situ* FTIR spectra recorded during ethanol oxidation, 0.5 mol L^{-1}, on Pt(111)/Rh/Sn in 0.1 mol L^{-1} **(B)** H_3PO_4, **(C)** $HClO_4$ and **(D)** H_2SO_4. The acetaldehyde band intensity occurs in 930 cm^{-1}.

Figures

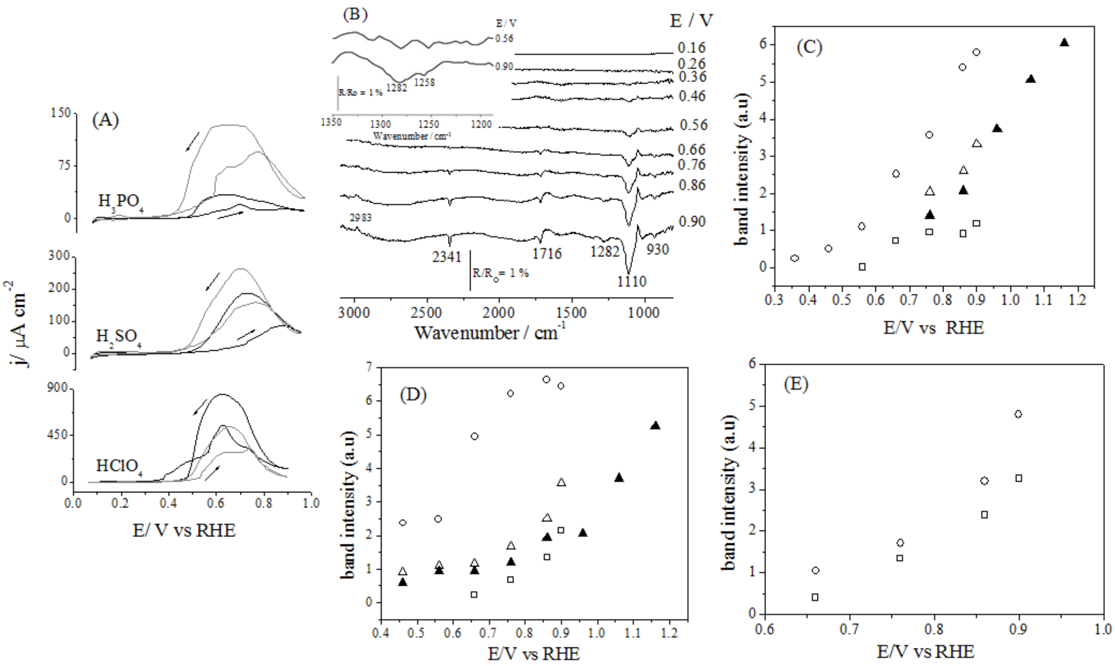
(A)
H3PO4
H2SO4
HClO4
j/ μA cm-2
E/ V vs RHE
(B)
E / V
0.16
0.26
0.36
0.46
0.56
0.66
0.76
0.86
0.90
2983
2341
1716
1282
1110
930
R/Ro = 1 %
Wavenumber / cm-1
1258
(C)
band intensity (a.u)
E/V vs RHE
(D)
(E)

Fig.1.

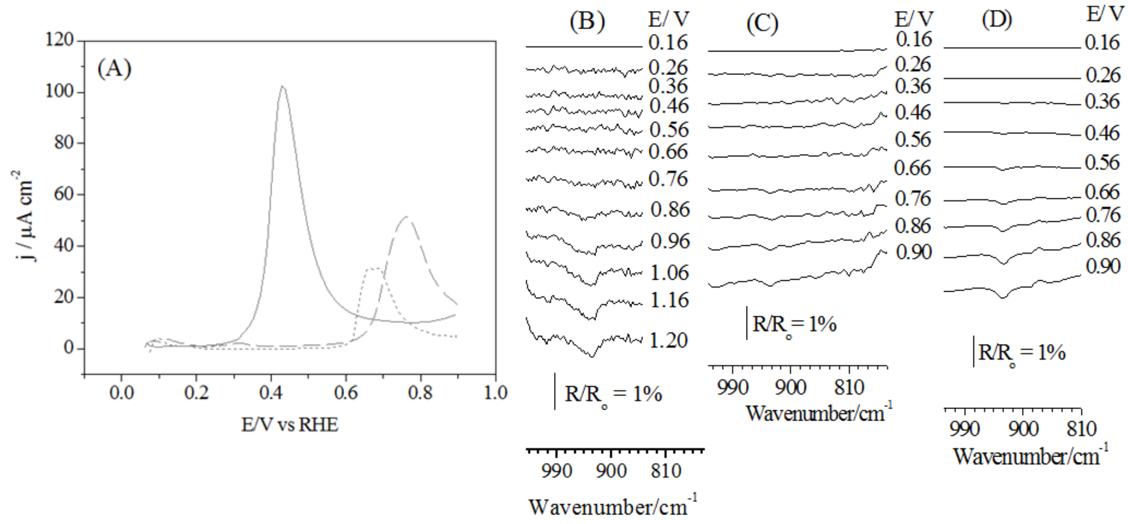
(A)
j / μA cm-2
E/V vs RHE
(B)
(C)
(D)
E/V
0.16
0.26
0.36
0.46
0.56
0.66
0.76
0.86
0.90
0.96
1.06
1.16
1.20
R/Ro = 1%
990
900
810
Wavenumber/cm-1

Fig. 2

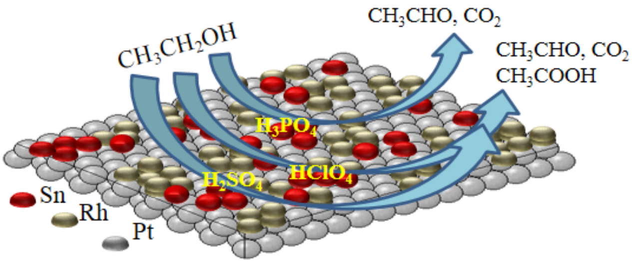

Graphical abstract

Highlights

- The effect of the anions, sulfate, perchlorate and phosphate, on ethanol electro-oxidation was demonstrated.
- The analysis was performed by in situ FTIR.
- Surface modified Pt (111) by Rh and Sn was used as electrode material.
- In situ FTIR spectroscopic data showed that H_2SO_4 is the most favorable to acetaldehyde and CO_2 formation.